JOURNAL OF CATALYSIS 65, 470–474 (1980)

NOTES

Pyridines by Propylene Ammoxidation: Catalyst Structure and Reaction Selectivity

In a previous study (*1*) it was observed that, within relatively large limits of composition, the performance of Te oxide/silica–alumina-based catalysts for the vapor-phase direct ammoxidation of propylene to pyridines strongly depends on the preparation procedure, so that our catalysts could be divided in two classes with respect to their selectivity. Reasonable quantities of the desired product were obtained only if silica–alumina was precipitated on preformed Te oxide or Te oxide–Sb oxide mixture. If the reverse process was followed, the solid obtained usually behaved only as a poor oxidation catalyst, and no pyridines or only small traces of such substances were found in the reactor effluent. The homogenization step, by milling in the presence of water, as described (*1*), generally proved to be useful, but did not substantially improve the performance of unselective catalysts. The selectivity to pyridines appeared to be connected with a particular structure which forms preferentially when the first preparation procedure is followed. Therefore, it seemed interesting to investigate to what extent the two classes of our catalysts are structurally different.

The chemical composition and catalytic behavior of some chosen solids, which typically represent the mentioned classes, are given in Table 1. Due to the preparation method (*1*), the Te oxide-based phase(s) was expected to be substantially crystalline, while the silica–alumina was expected to be practically amorphous. A polarizing optical microscope (POM) was then employed, at relatively low magnification, to detect structural macrodifferences. During the observations of the finely ground catalyst particles, the samples were immersed in chlorobenzene, in order to ensure a better transmittance of light. Some tens of different samples of each catalyst were observed and photographed, with the Nicol prisms of the POM (a Leitz SM-LUX microscope, equipped with a Canon EF camera) either in parallel or in perpendicular position, to reveal the presence of crystalline and amorphous phases, respectively. Typical results are shown in Fig. 1. One may observe that selective catalysts (Figs. 1a, b) show a macrostructure in which smaller particles of crystalline phases are completely embedded in an amorphous matrix. On the other hand, in unselective catalysts, small particles of amorphous phase appear to be surrounded by microparticles of crystalline phase(s) (Figs. 1c, d).

To obtain information about the composition of such different phases, a qualitative microanalysis was performed by scanning electron microscopy–electron probe microanalysis (SEM–EPMA) at higher magnifications. Many different specimens of each catalyst were prepared, by embedding the catalyst particles in Bakelite resin and cutting and polishing the surfaces of the

0021-9517/80/100470-05$02.00/0

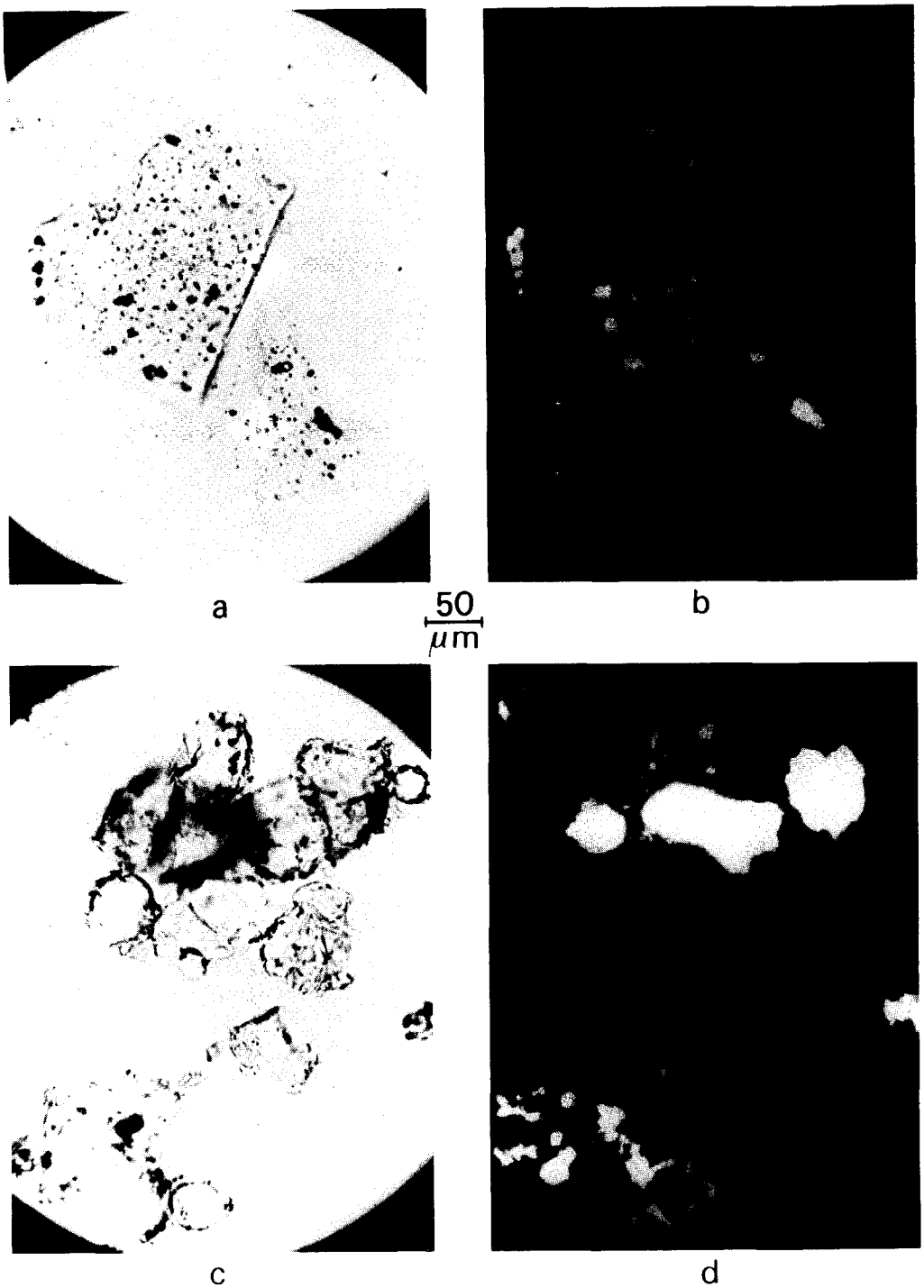

FIG. 1. Typical POM micrographs. (a, b) The same S-6 catalyst specimen but with ∥ and ⊥ Nicol prisms, respectively; (c, d) the same U-3 catalyst specimen with ∥ and ⊥ Nicol prisms, respectively.

TABLE 1

Catalyst Composition and Behavior[a]

Catalyst[b]	TeO_2 (wt%)	Sb_2O_3 (wt%)	SiO_2–Al_2O_3 (wt%)	C^c (mol%)	S_p[d]	Time factor (g h mol^{-1})
S-1	5.6	4.5	89.9	63.9	14.3	28.6
S-6	1.3	2.3	96.4	42.1	13.9	61.2
U-3	7.9	3.5	88.6	2.6	Tr	61.2

[a] Reaction conditions: 390°C; atmospheric pressure; molar ratios of fed reactants, $NH_3 : H_2O : C_3H_6$: air = 1 : 11 : 2 : 11.

[b] S = selective, U = unselective.

[c] Overall conversion of the olefin.

[d] mol% of converted olefin, transformed into pyridines; selectivity to other products (CO_2, acetaldehyde + acetone, acetonitrile + acrylonitrile, acetic acid, respectively): S-1, 25, 9.0, Tr, 7.5; S-6, 27, 4.9, Tr, 1.0; U-3, 80, 12.0, 5.5, Tr; balance by tar and coke; Tr = less than 0.1.

specimens with diamond paste, in the presence of various anhydrous lubricants (*2*). Typical results, obtained with a JEOL 50 A SEM–EPMA apparatus, are shown in Fig. 2. The structures of selective and of unselective catalysts again look different. The former show granules of Te oxide- and Sb oxide-based phases completely embedded in the silica-based phase (Figs. 2a–d), while the latter show a more uniform distribution of the Te oxide- and Sb oxide-rich phase(s) around the particles and very probably within the pores of the silica-based phase (Figs. 2e–h). EPMA performed by crossing the polished surface of the specimen along a given line (see, e.g., Fig. 2d) confirms such results. The same Fig. 2d seems also to show that, in S-1 catalyst (Table 1), the Te oxide-rich phase is less finely distributed in the silica–alumina matrix than is the Sb oxide-rich phase, at least in the specimens examined.

Apart from the minor differences in catalytic behavior, due to the different relative concentrations of the chemical components, the different performance of selective catalysts, with respect to unselective ones, seems to be connected with the presence of a silica-based acidic matrix, embedding small particles of the Te oxide-based phase(s).

The mechanism of the overall ammoxidation reaction to pyridines can therefore be imagined as follows. In the reaction conditions, the three gaseous reactants, i.e., propylene, oxygen, and ammonia, reach the external surface of the catalyst particles, but only propylene and oxygen can diffuse through the acidic silica–alumina, which would retain the basic ammonia. In such conditions, the formation of acrylonitrile-type products is virtually suppressed and the Te oxide-based catalyst can direct the oxidation of the olefin essentially toward aldehyde-type products. Such carbonyl compounds, counterdiffusing through the ammonia-loaded acidic phase, would then be converted to pyridines, as in the usual acid-catalyzed industrial synthesis of such heterocyclic substances from acetaldehyde and ammonia (*3*). When the catalyst structure is inverted, i.e., when the oxidation

FIG. 2. Typical SEM–EPMA photomicrographs. (a, b, and c) The same S-6 catalyst specimen: SEM image, Si$K\alpha$ and Sb$L\alpha_1$ EPMA maps, respectively; (d) S-1 catalyst specimen, SEM image with crossing-line EPMA traces: (1) position of Te$L\alpha_1$ line (upper trace), (2) position of Sb$L\alpha_1$ line (lower trace); (e, f, g, and h) the same U-3 catalyst specimen: SEM image, Si$K\alpha$, Te$L\alpha_1$, and Sb$L\alpha_1$ EPMA maps, respectively. (a–c, 1800×; d–h, 1000×.)

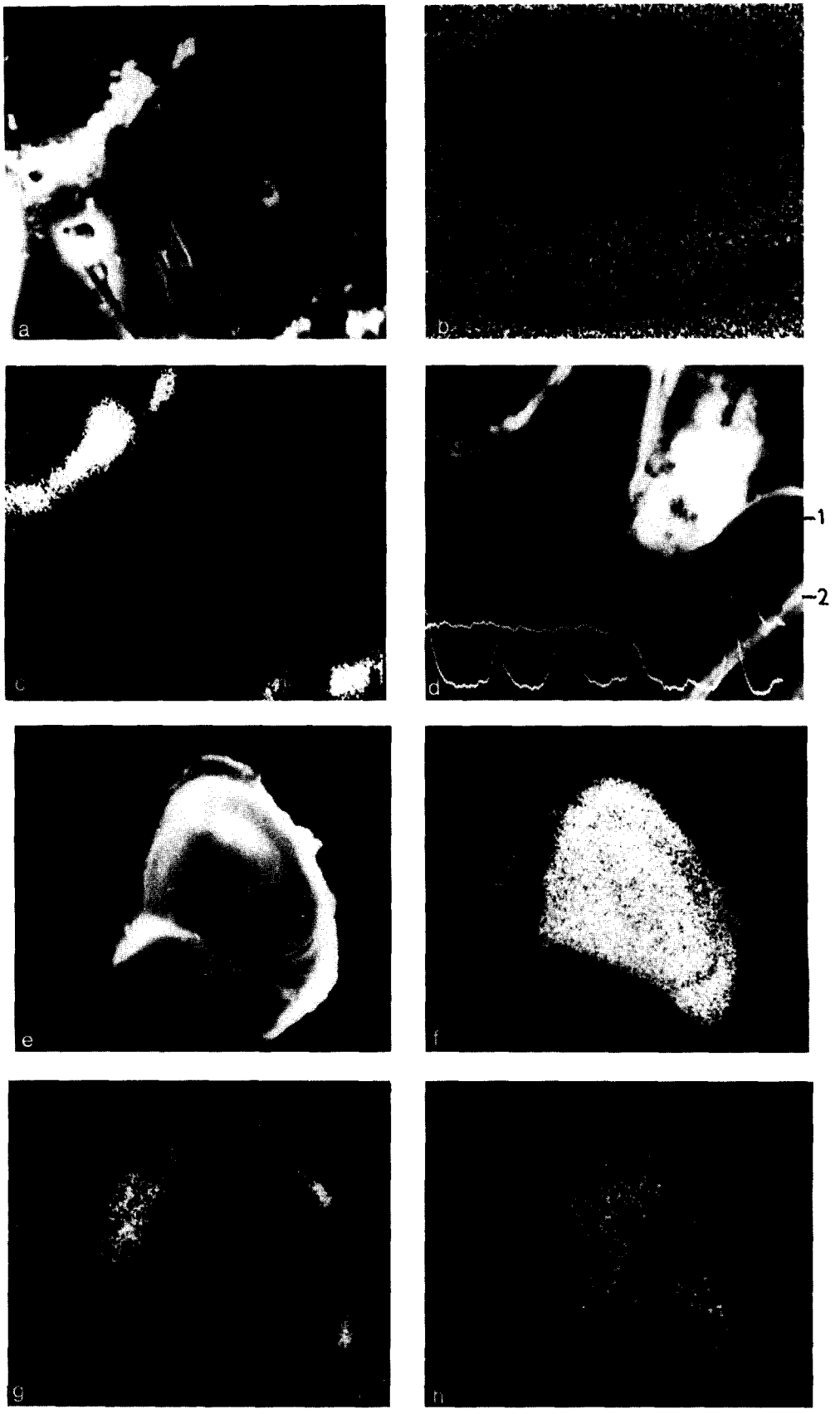

FIG. 2

catalyst encapsulates the acidic phase, the system is poorly selective, probably because the presence of the ammonia, during the oxidation of the olefin, directs the reaction mainly toward nitrile-type products, which cannot any more be transformed into pyridine-type substances, and because carbonyl compounds, formed on the external oxidizing phase can easily desorb rather than diffuse toward the less accessible internal acidic phase.

ACKNOWLEDGMENTS

The financial aid of the Italian Consiglio Nazionale delle Richerche is gratefully acknowledged.

REFERENCES

1. Forni, L., and Stanga, M., *J. Catal.* **59**, 148 (1979).
2. Anderson, R. B., and Dawson, P. T. (Eds.), *in* "Experimental Methods in Catalytic Research," Vol. 2, Chaps. 3 and 4. Academic Press, New York, 1976.
3. Kirk, R. E., and Othmer, D. F., (Eds.), *in* "Encyclopedia of Chemical Technology," 2nd ed., Vol. 16, p. 780. Wiley, New York, 1968.

LUCIO FORNI
MARIO TESCARI[1]
PIERINO ZAMBELLI[1]

Instituto di Chimica Fisica
e Centro CNR
Università di Milano
Via Golgi 19
20133 Milan, Italy

Received November 26, 1979; revised March 21, 1980

[1] Euteco Impianti S.p.A., Paderno D., Milan, Italy.